Tetradecker Metallacarborane Sandwiches: Synthesis via Double-Decker Stacking and Structural Characterization of Co–Co–Co, Co–Ni–Co, and Co–Ru–Co Complexes[1]

Kent W. Piepgrass, Xiangsheng Meng, Markus Hölscher,† Michal Sabat, and Russell N. Grimes*

Department of Chemistry, University of Virginia, Charlottesville, Virginia 22901

Received August 25, 1992

Stacking reactions of the bridge-deprotonated $Cp^*Co(2,3\text{-}Et_2C_2B_3H_3\text{-}5\text{-}X)^-$ complexes (**1a–1f**; X = Cl, Br, CH_3, $C(O)CH_3$, $CH_2C{\equiv}CCH_3$, H; $Cp^* = \eta^5\text{-}C_5Me_5$) with cobalt(II) and nickel(II) halides in THF gave, respectively, diamagnetic $[Cp^*Co^{III}(Et_2C_2B_3H_2X)]_2Ni^{IV}$ (**2a–2e**) and paramagnetic $[Cp^*Co^{III}(Et_2C_2B_3H_2X)]_2Co^{IV}$ (**3a–3f**) tetradecker sandwich complexes. A similar reaction of the *B*(5)-chloro reagent **1a** using $RuCl_2$ gave the diamagnetic trichloro complex $(Cp^*Co)_2(2,3\text{-}Et_2C_2B_3H_2\text{-}5\text{-}Cl)(2,3\text{-}Et_2C_2B_3H\text{-}4,5[5,6]\text{-}Cl_2)Ru$ (**4**). In all cases except the Co–Co–Co compound **3f** (X = H), the products were isolated as dark crystalline solids via chromatography on silica; **3f** decomposes on silica and was isolated via fractional crystallization from a cold solution. All of the tetradeckers are air-stable in the solid state and in solution except **3f**, which is stable only as a solid. Characterization of these compounds was based on ^1H, ^{11}B, and ^{13}C NMR (for diamagnetic species), UV–visible, and mass spectra, supported by X-ray crystallographic data on the Co–Ni–Co and Co–Co–Co dichloro compounds (**2a** and **3a**), the Co–Ni–Co diacetyl complex (**2d**), and the Co–Ru–Co sandwich **4**. The structurally characterized compounds are tetradecker sandwiches, slightly bent in the middle (8–15°) but exhibiting no significant ring slippage relative to the coordinated metal atoms. The carborane rings in these sandwiches are mutually rotated by 27–89°. The electronic spectra exhibit intense absorption bands between 350 and 440 nm with extinction coefficients between 28 000 and 43 000 $M^{-1}\,cm^{-1}$. The molecular geometries and spectroscopic properties of the tetradeckers can be qualitatively correlated with published molecular orbital calculations on the ideal $Cp_4Co_3^+$ tetradecker system. The formation and stabilization of the tetradecker complexes is favored by precursor complexes (e.g., **1a–1f**) having relatively electron-withdrawing X substituents, as measured by the shift to low field of the ^1H NMR B–H–B signal. Crystal data for **2a**: mol wt 751.1; space group $P2_1$; $Z = 2$; $a = 9.018$ (3), $b = 19.433$ (5), $c = 10.592$ (2) Å; $\beta = 100.79$ (2)°; $V = 1823$ Å^3; $R = 0.031$ for 3877 reflections having $I > 3\sigma(I)$. Crystal data for **3a** (isomorphous with **2a**): mol wt 751.3; $a = 9.053$ (2), $b = 19.246$ (5), $c = 10.651$ (3) Å; $\beta = 100.47$ (2)°. Crystal data for **2d**: mol wt 840.3; space group $P\bar{1}$; $Z = 2$; $a = 10.490$ (4), $b = 13.034$ (6), $c = 17.531$ (7) Å; $\alpha = 106.52$ (1), $\beta = 97.70$ (1), $\gamma = 108.83$ (1)°; $V = 2107$ Å^3; $R = 0.070$ for 3494 reflections having $I > 2\sigma(I)$. Crystal data for **4**: mol wt 827.9; space group *Pbca*; $Z = 8$; $a = 23.254$ (6), $b = 18.068$ (2), $c = 17.338$ (4) Å; $V = 7285$ Å^3; $R = 0.032$ for 4171 reflections having $I > 3\sigma(I)$.

Introduction

Multidecker metal sandwich complexes are of interest from both theoretical and practical perspectives[2]—for example, as potential building blocks for low-dimensional electroactive polymers—and the development of rational methods for their synthesis is an important objective in organometallic chemistry. In our laboratory, efforts in this area date from the preparation 20 years ago of $CpCo(C_2B_3H_5)CoCp$ isomers, the first neutral, stable triple-decker sandwiches.[3] More recently, our group has characterized a series of triple-deckers containing Co, Fe, Ni, Ru, Rh, or Os, including dimeric and oligomeric linked complexes.[4] In addition to these carborane-based species, further examples of true (nonslipped) triple-decker sandwiches employing organoborane,[5] hydrocarbon,[6] or other (e.g. P_n and As_n[7]) ring ligands have been prepared by other groups.

Far less is known of larger stacked complexes. Siebert and co-workers have prepared several tetradeckers,[5a,b] a pentadecker,[8] a hexadecker,[9] and a partially characterized, semiconducting stacked polymer,[10] all of which incorporate diborolenyl (C_3B_2) or thiadiborolenyl (C_2SB_2) bridging rings. Recently, our two groups collaborated in the preparation of several hybrid-tetradecker sandwiches containing both carboranyl and diborolenyl ligands,[11] but tetradeckers having only carborane bridges remained an elusive target. A seemingly obvious route to such

† Visiting research student from the Institut für Anorganische Chemie, Technischen Hochschule Aachen, Aachen, Germany, 1990.

(1) Organotransition-Metal Metallacarboranes. 30. (a) Part 29: Benvenuto, M. A.; Sabat, M.; Grimes, R. N. *Inorg. Chem.* **1992**, *31*, 3904. (b) Part 28: Benvenuto, M. A.; Grimes, R. N. *Inorg. Chem.* **1992**, *31*, 3897.

(2) Some pertinent reviews include the following: (a) Marks, T. J. *Angew. Chem., Int. Ed. Engl.* **1990**, *29*, 857. (b) Burdett, J. K.; Canadell, E. *Organometallics* **1985**, *4*, 805. (c) Grimes, R. N. *Chem. Rev.* **1992**, *92*, 251.

(3) (a) Beer, D. C.; Miller, V. R.; Sneddon, L. G.; Grimes, R. N.; Mathew, M.; Palenik, G. J. *J. Am. Chem. Soc.* **1973**, *95*, 3046. (b) Grimes, R. N.; Beer, D. C.; Sneddon, L. G.; Miller, V. R.; Weiss, R. *Inorg. Chem.* **1974**, *13*, 1138.

(4) (a) Davis, J. H., Jr.; Sinn, E.; Grimes, R. N. *J. Am. Chem. Soc.* **1989**, *111*, 4776. (b) Davis, J. H., Jr.; Sinn, E.; Grimes, R. N. *J. Am. Chem. Soc.* **1989**, *111*, 4784. (c) Davis, J. H., Jr.; Benvenuto, M.; Grimes, R. N. *Inorg. Chem.* **1991**, *30*, 1765. (d) Chase, K. J.; Bryan, R. F.; Woode, M. K.; Grimes, R. N. *Organometallics* **1991**, *10*, 2631.

(5) (a) Siebert, W. *Angew. Chem., Int. Ed. Engl.* **1985**, *24*, 943; *Pure Appl. Chem.* **1987**, *59*, 947 and references therein. (b) Wadepohl, H. Dissertation, University of Marburg, Germany, 1982. (c) Herberich, G. E.; Hessner, B.; Huttner, G.; Zsolnai, L. *Angew. Chem., Int. Ed. Engl.* **1981**, *20*, 472. (d) Wörner, K.-F.; Uhm, J.-K.; Pritzkow, H.; Siebert, W. *Chem. Ber.* **1990**, *123*, 1239.

(6) (a) Werner, H.; Salzer, A. *Synth. React. Inorg. Met.-Org. Chem.* **1972**, *2*, 239. (b) Duff, A. W.; Jonas, K.; Goddard, R.; Kraus, H.-J.; Krueger, C. *J. Am. Chem. Soc.* **1983**, *105*, 5479. (c) Kudinov, A. R.; Rybinskaya, M. I.; Struchkov, Yu. T.; Yanovskii, A. I.; Petrovskii, P. V. *J. Organomet. Chem.* **1987**, *336*, 187. (d) Lumme, P. O.; Turpeinen, U.; Kudinov, A. R.; Rybinskaya, M. I. *Acta Crystallogr.* **1990**, *C46*, 1410. (e) Schneider, J. J.; Goddard, R.; Werner, S.; Krüger, C. *Angew. Chem., Int. Ed. Engl.* **1991**, *30*, 1124. (f) Cotton, F. A.; Kibala, P. A.; Wojtczak, J. *J. Am. Chem. Soc.* **1991**, *113*, 1142.

(7) Scherer, O. J. *Angew. Chem., Int. Ed. Engl.* **1990**, *29*, 1104 and references therein.

(8) Whiteley, M. W.; Pritzkow, H.; Zenneck, U.; Siebert, W. *Angew. Chem., Int. Ed. Engl.* **1982**, *21*, 453.

(9) Kuhlmann, T.; Siebert, W. *Z. Naturforsch.* **1985**, *40B*, 167.

(10) Siebert, W. *Pure Appl. Chem.* **1988**, *60*, 1345.

(11) Fessenbecker, A.; Attwood, M. D.; Grimes, R. N.; Stephan, M.; Pritzkow, H.; Zenneck, U.; Siebert, W. *Inorg. Chem.* **1990**, *29*, 5164.

0020-1669/92/1331-5202$03.00/0

Scheme I

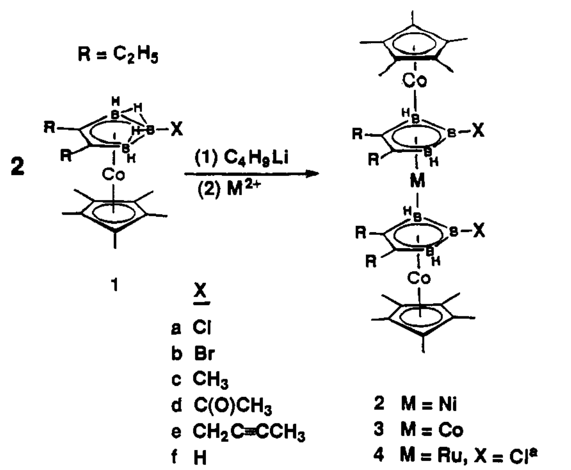

species—the stacking of two double-decker $CpMC_2B_3$ units around a third metal (Scheme I)—was attractive, given the readily accessible *nido*-LM($Et_2C_2B_3H_5$) complexes (L = Cp, Cp* [Cp* = η^5-C_5Me_5], arene; M = Fe, Co, Ru),[4a,12] which can now be obtained on a multigram scale. However, in our hands attempted reactions of this type failed to give isolable tetradecker products until we found, serendipitously, that success can be achieved by employing Cp*Co($Et_2C_2B_3H_4$-5-X) double-deckers having an appropriate X substituent on the middle boron. We have published a preliminary report on this finding[13] and here present a full account of the synthetic studies together with structural characterization of several tetradecker products.

Results and Discussion

Synthesis. The double-decker stacking sequence shown in Scheme I was employed with a series of B(5)-substituted Cp*Co-($Et_2C_2B_3H_4X$) complexes (**1a**–**1e**), which are yellow, air-stable crystalline solids prepared via derivatization of the Cp*Co-($Et_2C_2B_3H_5$) parent compound (**1f**).[14] Bridge-deprotonation of these neutral complexes with butyllithium in THF immediately generated a red or orange monoanion. Upon addition of a metal halide, formation of a tetradecker was signaled by a color change initially to brown and then to nearly black. Isolation and purification of the products via chromatography in air on silica gel columns and preparative-scale plates gave the diamagnetic Co^{III}-Ni^{IV}-Co^{III} complexes **2a**–**2e** and the paramagnetic Co^{III}-Co^{IV}-Co^{III} species **3a**–**3e**. (The corresponding *B,B'*-diiodo Co–Co–Co tetradecker has been prepared in a similar manner from Cp*Co($Et_2C_2B_3H_4$-5-I) and CoI_2).[15] The formation of these products clearly involves not only the initial metal complexation of the double-decker substrates but also the workup on silica in air; at least some of the metal oxidation, and possibly other changes, probably occurs during this latter stage. Indeed, the isolation of the unsubstituted tricobalt complex **3f**, described below, was possible only by avoiding contact with silica. Hence, in general a simple stoichiometric description of the tetradecker formation cannot be given.

(12) (a) Maynard, R. B.; Swisher, R. G.; Grimes, R. N. *Organometallics* **1983**, *2*, 500. (b) Swisher, R. G.; Grimes, R. N. *Organomet. Synth.* **1986**, *3*, 104. (c) Swisher, R. G.; Sinn, E.; Grimes, R. N. *Organometallics* **1983**, *2*, 506; **1985**, *4*, 896.
(13) Piepgrass, K. W.; Davis, J. H., Jr.; Sabat, M.; Grimes, R. N. *J. Am. Chem. Soc.* **1991**, *113*, 681.
(14) (a) Davis, J. H., Jr.; Attwood, M. D.; Grimes, R. N. *Organometallics* **1990**, *9*, 1171. (b) Piepgrass, K. W.; Grimes, R. N. *Organometallics* **1992**, *11*, 2397. (c) Piepgrass, K. W.; Stockman, K. E.; Sabat, M.; Grimes, R. N. *Organometallics* **1992**, *11*, 2404.
(15) Piepgrass, K. W.; Curtis, M. A.; Meng, X.; Wang, X.; Sabat, M.; Grimes, R. N. Manuscripts in preparation.

Similar treatment of the *B(5)*-chloro reagent **1a** using $RuCl_2$ generated the diamagnetic trichloro Co–Ru–Co complex $(Cp^*Co)_2$(2,3-$Et_2C_2B_3H_2$-5-Cl)(2,3-$Et_2C_2B_3H$-4,5[5,6]-Cl_2)-Ru (**4**). The addition of a third chlorine to this complex presumably occurred during workup in dichloromethane, a frequent observation in this area of chemistry.[4a] All of the tetradeckers isolated thus far are intensely colored and appear black in crystalline form, and (except for **3f**) are air-stable in solution and the solid state. Characterization of these compounds is based on ^1H, ^{11}B, and ^{13}C NMR (for diamagnetic species), UV–visible, and mass spectra (Tables I and II and Experimental Section), supported by X-ray crystallographic data on **2a**, **2d**, **3a**, and **4**.

Many other Cp*Co($Et_2C_2B_3H_4$-5-X) derivatives failed to generate isolable tetradecker complexes via the reaction sequence just described—such products either not forming at all, or undergoing subsequent reaction—and it was apparent that the choice of the X substituent is a determining factor in obtaining stable tetradecker systems. Thus, although the *B(5)*-acetyl derivative **1d** readily undergoes stacking to give **2d** and **3d**, the *B(5)*-ethyl species is unreactive; indeed, treatment of the Cp*Co($Et_2C_2B_3H_3$-5-Et)$^-$ anion with $NiBr_2$ or $CoCl_2$ failed even to produce a noticeable color change, a clear indication that no tetradecker stacking occurred. (The corresponding *B(5)*-CH_2-OMe and *B(5)*-CH_2Ph derivatives behaved similarly.) These findings early in our study suggested that the formation of tetradecker sandwiches is promoted by the presence of electron-withdrawing groups on the carborane ring ligands, a hypothesis that received further support from the synthesis of chloro-, bromo-, and propargyl-substituted Ni and Co tetradeckers. Moreover, in general the highest isolated yields of tetradecker products were obtained from the substrates bearing the most strongly electron-withdrawing substituents, viz., Cl, Br, and acetyl.

The electronic influence of the *B(5)*-X functional group on the stacking reaction can be correlated with the B–H–B signal in the ^1H spectra of the Cp*Co($Et_2C_2B_3H_4$-5-X) precursor, which is sensitive to the nature of X. As shown in Table III, a clear demarcation appears between those species having B–H–B shifts deshielded relative to δ −5.25, which generate isolable tetradeckers under the conditions described above, and those with more negative values, which thus far have not been found to do so. Additionally, the significance of these shifts as empirical indicators of electron-withdrawal from the C_2B_3 face is underlined by the fact that δ is most deshielded for X = Cl and Br. Although the methyl group is not normally considered electron-withdrawing, the relatively low-field shift of δ −5.23 exhibited by the *B(5)*-methyl derivative (which remarkably is deshielded by 0.13 ppm relative to the ethyl species) suggested that tetradecker formation might be possible with that complex. This was indeed the case, as was demonstrated by the isolation of the nickel and cobalt *B(5)*,*B(5')*-dimethyl species **2c** and **3c**.

As noted earlier, the failure to isolate a specific tetradecker may indicate either that it does not form at all or that it is initially generated but subsequently converts to other species on exposure to air or silica. In the latter case, tetradeckers that do not survive the normal workup procedure might be isolated by alternative methods. Pursuing this idea, we have found that the parent Co–Co–Co tetradecker **3f**, a previously unobtainable species, is indeed produced under the same conditions as **3a**–**3e** and can be isolated via fractional crystallization from solution while avoiding contact with silica or atmospheric oxygen. Thus, while the high-field (δ −5.94) B–H–B proton NMR shift of parent Cp*Co($Et_2C_2B_3H_5$) correlates with the instability of the tetradecker product **3f** on silica columns, it clearly does not preclude formation of that species in solution. This implies that additional tetradeckers might be prepared from other double-decker complexes "below the line" in Table III and isolated in a similar fashion, but none has been found as yet. Of particular interest is the *B(5)*-ethyl derivative

Table I. ^{11}B, ^{1}H, and ^{13}C FT NMR Data

115.8-MHz ^{11}B NMR Data

compd	$\delta^{a,b}$	rel areas
$[(C_5Me_5)Co(2,3\text{-}Et_2C_2B_3H_2\text{-}5\text{-}Cl)]_2Ni$ (**2a**)	77.5, 6.8	1:2
$[(C_5Me_5)Co(2,3\text{-}Et_2C_2B_3H_2\text{-}5\text{-}Br)]_2Ni$ (**2b**)	70.7, 10.6	1:2
$[(C_5Me_5)Co(2,3\text{-}Et_2C_2B_3H_2\text{-}5\text{-}Me)]_2Ni$ (**2c**)	84.7, 7.7	1:2
$[(C_5Me_5)Co(2,3\text{-}Et_2C_2B_3H_2\text{-}5\text{-}C(O)Me)]_2Ni$ (**2d**)	65.6, 11.8	1:2
$[(C_5Me_5)Co(2,3\text{-}Et_2C_2B_3H_2\text{-}5\text{-}CH_2C{\equiv}CMe)]_2Ni$ (**2e**)	77.5, 10.4	1:2
$[(C_5Me_5)Co]_2(2,3\text{-}Et_2C_2B_3H_2\text{-}5\text{-}Cl)(2,3\text{-}Et_2C_2B_3H\text{-}4,5[5,6]\text{-}Cl_2)Ru$ (**4**)	85.9, 79.7, 60.5, 57.6, 28.6, 22.8	1:1:1:1:1:1

300-MHz ^{1}H NMR Data

compd	δ^{c-e}
2a	2.38 q (ethyl CH_2), 1.48 s (C_5Me_5), 1.41 t (ethyl CH_3)
2b	2.42 q (ethyl CH_2), 1.49 s (C_5Me_5), 1.42 t (ethyl CH_3)
2c	2.37 q (ethyl CH_2), 1.47 s (C_5Me_5), 1.38 t (ethyl CH_3), 1.28 s (B–CH_3)
2d	2.44 s ($C(O)CH_3$), 2.30 q (ethyl CH_2), 1.40 s (C_5Me_5), 1.38 t (ethyl CH_3)
2e	2.79 sb (B–CH_2?), 2.39 q (ethyl CH_2), 1.94 s (butynyl CH_3), 1.49 s (C_5Me_5), 1.42 t (ethyl CH_3)
4	2.87 m (ethyl CH_2), 2.61 m (ethyl CH_2), 2.48 m (ethyl CH_2), 2.20 m (ethyl CH_2), 1.66 s (C_5Me_5), 1.65 s (C_5Me_5), 1.32 t (ethyl CH_3), 0.99 t (ethyl CH_3), 0.87 t (ethyl CH_3), 0.71 t (ethyl CH_3)

75.5-MHz ^{13}C NMR Data

compd	$\delta^{c,f}$
2a	102.4 (C_2B_3), 90.0 (C_5 ring), 24.3 (ethyl CH_2), 15.3 (ethyl CH_3), 9.9 (C_5Me_5 CH_3)
2b	101.8 (C_2B_3), 89.9 (C_5 ring), 24.5 (ethyl CH_2), 15.4 (ethyl CH_3), 9.4 (C_5Me_5 CH_3)
2c	99.9 (C_2B_3), 88.8 (C_5 ring), 24.0 (ethyl CH_2), 15.4 (ethyl CH_3), 13.7 (B–CH_3), 9.6 (C_5Me_5 CH_3)
2d	103.0 (C_2B_3), 90.0 (C_5 ring), 37.9 (acetyl CH_3), 24.5 (ethyl CH_2), 15.2 (ethyl CH_3), 9.5 (C_5Me_5 CH_3)

[a] Shifts relative to $BF_3{\cdot}OEt_2$, positive values downfield. H–B coupling was not resolved. [b] 1:1 dichloromethane–*n*-Hexane solution. [c] $CDCl_3$ solution. [d] Shifts relative to $(CH_3)_4Si$. Integrated peak areas in all cases are consistent with the assignments given. Legend: m = multiplet, s = singlet, sb = broad singlet, d = doublet, t = triplet, q = quartet. [e] B–$H_{terminal}$ resonances are broad quartets and are mostly obscured by other signals. [f] Shifts relative to $(CH_3)_4Si$; all spectra proton-decoupled.

Table II. Electronic Absorption Spectra of Tetradecker Complexes[a]

compd	metal system	substituent groups	λ^b	ϵ^c
2a	Co–Ni–Co	Cl, Cl	436	28500
			332	9400
2c	Co–Ni–Co	Me, Me	494 (sh)	9500
			422	43100
			374 (sh)	28600
			378 (sh)	26000
			298	21600
2d	Co–Ni–Co	C(O)Me, C(O)Me	574 (sh)	6700
			432	35200
			322 (sh)	21000
			308	26000
3a	Co–Co–Co	Cl, Cl	418	36700
			312	22100
3b	Co–Co–Co	Br, Br	412	35300
			306	24700
3c	Co–Co–Co	Me, Me	540 (sh)	5400
			400	30100
			374 (sh)	28400
			308	22500
3e	Co–Co–Co	$CH_2C{\equiv}CMe$, $CH_2C{\equiv}CMe$	406	33200
			360	25000
			300	23800
3f	Co–Co–Co	H, H	554 (sh)	2300
			356	32600
			318	31600
4	Co–Ru–Co	Cl, Cl_2	812	4000
			484	12100
			366	40900
			308	21200

[a] In CH_2Cl_2 solution. [b] Wavelength in nm; sh = shoulder. [c] Extinction coefficients in M^{-1} cm^{-1}.

mentioned earlier, which has given no evidence of tetradecker sandwich formation under any conditions investigated.

The interaction of $Cp^*Co(Et_2C_2B_3H_3X)^-$ ions with metal halides in THF solution is complex, and the formation of tetradeckers competes with other reactions, including (1) protonation of the ion to regenerate the neutral complex,[14] (2) dimerization of the ion via oxidative coupling or linkage,[15] and (3) metal-promoted oxidative fusion to produce open 12-vertex $Co_2C_4B_6$ clusters[15,16] (a process that may well involve tetradecker-like intermediates). The products actually isolated from these systems may reflect any or all of these processes, and as we have just seen, the methods of separation applied during workup can further affect the nature and distribution of isolated species. Side reactions of types 1–3 can lower the yield of tetradecker complexes, and under some conditions these predominate; several systems in which this is the case have been investigated and will be described elsewhere.[15] In the present context, we focus on the characterization of the tetradecker sandwiches. From our observations

Table III. B–H–B Proton NMR Shifts of $(C_5Me_5)Co(2,3\text{-}Et_2C_2B_3H_4\text{-}5\text{-}X)$ Complexes

X	δ^b	X	δ^b
Complexes Forming Isolable Tetradeckers[a]			
Cl	–3.98	$CH_2C{\equiv}CMe$	–5.15
Br	–4.22	C(O)Me	–5.20
I	–4.60	Me	–5.23
$C({=}CH_2)OC(O)Me^c$	–4.90		
Other Complexes[d]			
$CH_2C{\equiv}CCH_2Cl$	–5.25	$CH_2C_6F_5$	–5.42
$CH_2C_6H_5$	–5.27	$CH_2C_2H_5$	–5.46
CH_2OMe	–5.31	$CHMe_2$	–5.55
$CH_2C(O)OH$	–5.29	CH_2CN	–5.41
$CH_2C(O)NH_2$	–5.30	$CH_2CH_2NH_2$	–5.50
CH_2OH	–5.31	$CH_2C(O)Me$	–5.54
$CH_2OC(O)Me$	–5.34	CH_2CF_3	–5.58
$CH_2C(O)OEt$	–5.34	CN	–5.60
$CH_2CH{=}CH_2$	–5.36	CH_2CH_2CN	–5.67
Et	–5.36	H[e]	–5.94[f]

[a] Based on reactions of bridge-deprotonated anions with $CoCl_2$ or $NiBr_2$ in THF, under conditions described in text. [b] Data taken from ref 14a–c; 300-MHz ^1H FT NMR spectra in $CDCl_3$ solution. B–H–B signals are broad singlets. [c] Formed *B*(5),*B*(5′)-diacetyl) tetradecker (see ref 14c). [d] Tetradecker synthesis has been attempted with some but not all of these complexes. [e] Tetradecker complex was formed, but was unstable on silica and was isolated via fractional crystallization (see text). [f] Incorrectly reported as –5.54 in ref 4a.

(16) Grimes, R. N. *Adv. Inorg. Chem. Radiochem.* **1983**, *26*, 55. Wong, K.-S.; Bowser, J. R.; Pipal, J. R.; Grimes, R. N. *J. Am. Chem. Soc.* **1978**, *100*, 5045. Pipal, J. R.; Grimes, R. N. *Inorg. Chem.* **1979**, *18*, 1936.

Table IV. Experimental X-ray Diffraction Parameters and Crystal Data

	2a (**3a**[a])	**2d**	**4**
empirical formula	$NiCo_2Cl_2C_{32}B_6H_{54}$	$NiCo_2Cl_{1.75}O_2C_{37}B_6H_{60}$	$RuCo_2Cl_3C_{32}B_6H_{53}$
fw	751.1	840.3	827.9
cryst color, habit	black prism	dark brown plate	black plate
cryst dimens, mm	0.43 × 0.38 × 0.32	0.20 × 0.20 × 0.05	0.48 × 0.32 × 0.30
space group	$P2_1$	$P\bar{1}$	*Pbca*
a, Å	9.018 (3)	10.490 (4)	23.254 (6)
b, Å	19.433 (5)	13.034 (6)	18.068 (2)
c, Å	10.592 (2)	17.531 (7)	17.338 (4)
α, deg	90.00	106.52 (1)	90.00
β, deg	100.79 (2)	97.70 (1)	90.00
γ, deg	90.00	108.83 (1)	90.00
V, Å^3	1823	2107	7285
Z	2	2	8
μ, cm^{-1} (Mo Kα)	15.81	13.64	15.46
transm factors	0.89–1.00	0.81–1.00	0.89–1.00
D(calcd), g cm^{-3}	1.368	1.325	1.510
$2\theta_{max}$, deg	55	45	50
no. of reflcns measd	4262	5275	7065
no. of reflcns obsd	3877[b]	3494[c]	4171[b]
R	0.031	0.070	0.032
R_w	0.042	0.075	0.047
largest peak in final diff map, e/Å^3	0.32	0.61	0.59

[a] Lattice parameters for **3a** (isomorphous with **2a**) are as follows: a = 9.053 (2) Å, b = 19.246 (5) Å, c = 10.651 (3) Å, β = 100.47 (2)°. [b] $I > 3\sigma(I)$. [c] $I > 2\sigma(I)$.

thus far, it appears that the presence of an electron-withdrawing substituent on the C_2B_3 ring effectively reduces the reactivity of both double-decker and tetradecker complexes toward electrophiles, thereby inhibiting side reactions of the types mentioned and also stabilizing the tetradecker products.

Spectroscopic Characterization of Tetradecker Sandwiches. The mass spectra of all products exhibit intense parent groupings, with little fragmentation in most cases. The NMR signals of the paramagnetic Co–Co–Co compounds **3a**–**3f** are broad and generally uninterpretable, but those of the diamagnetic Co–Ni–Co series **2a**–**2e** (Table I) are consistent with tetradecker sandwich geometry. The low-field area-1 ^{11}B NMR signals (δ ca. 66–86 ppm), arising from the middle boron atoms, are characteristic of complexes containing planar 2,3-C_2B_3 rings that are sandwiched between two transition metals (and hence are a feature of carborane triple-decker as well as tetradecker complexes).[3,4] The less symmetrical Co–Ru–Co complex **4**, which contains inequivalent carborane rings, exhibits a more complex spectrum indicating six boron environments, consistent with the X-ray structure determination discussed below. The ^{13}C NMR spectra exhibit unusually sharp peaks corresponding to the C_2B_3 ring carbons with δ values near 100 ppm, significantly deshielded relative to the C_5Me_5 ring carbon atoms.

The X-band ESR spectrum of the dichloro Co–Co–Co complex **3a** at −170 K in toluene gave $g_{\parallel}$ and $g_{\perp}$ values of 2.37 and 2.035, respectively, with no resolved cobalt hyperfine structure. The spectrum resembles those of previously studied double-decker Fe(III) complexes having a **g** tensor of axial symmetry and of paramagnetic Co–Ni diborolenyl-bridged triple-decker complexes, which show a very small cobalt hyperfine splitting.[17] It is evident that the three cobalt centers in **3a** are inequivalent, and on this basis it might be argued that electron delocalization is not extensive; on the other hand, detailed electrochemical studies of **3a** and other paramagnetic tetradecker complexes, to be reported elsewhere,[18] are consistent with delocalized electronic structures for these systems. It is also relevant to note that the closely related C_2B_3-bridged cationic Co–Co and Co–Ru triple-decker sandwiches have been shown to be fully delocalized (Robin and Day Class III) mixed-valent species.[19]

The UV–visible spectra of the tetradecker complexes (Table II) contain strong absorption bands with maxima between ca. 350 and 440 nm and extinction coefficients in the range of 28 000–43 000 M^{-1} cm^{-1}. The absorptions in the visible region are sufficiently strong to produce intense, nearly black coloration in the solid crystals. These spectra contrast sharply with those of their pale yellow or yellow-orange precursor double-decker complexes[14b,c] **1a**–**1f** and indicate strong electronic interaction between the central M^{4+} ion and two $Cp^*Co(Et_2C_2B_3H_3)^{2-}$ sandwich units. Thus, the high observed ε values are consistent with charge-transfer excitations involving bonding MOs on the ligands and empty antibonding orbitals on M. This model can be correlated with a theoretical study[20] of tetradecker sandwiches that employed the hypothetical $CpCoCpCoCpCoCp^+$ model system, a 46-electron sandwich in which the strongly antibonding $3e_{1g}$ HOMO is occupied by 4 electrons. In our Co–Ni–Co, Co–Co–Co, and Co–Ru–Co tetradeckers, which have, respectively, 42, 41, and 40 valence electrons, the orbitals corresponding to the $3e_{1g}$ (which will be nondegenerate owing to the lower symmetry introduced by the carborane ring ligands) are empty and hence are the LUMOs in these species. The HOMOs in our systems therefore would correspond to the a_{1g} or $2e_{1u}$ MOs in the idealized $CpCoCpCoCpCoCp^+$ sandwich,[20] which are of much lower energy than the $3e_{1g}$ MO. This model predicts a large HOMO–LUMO energy gap in our systems, which is consistent with the short wavelengths of the absorbances and with the suggested charge-transfer nature of the transitions. More detailed analysis of the electronic spectra will require quantitative MO calculations on the C_2B_3-bridged tetradecker stacks, which are not yet available.

X-ray Crystallographic Studies. Data were collected on the dichloro and diacetyl Co–Ni–Co complexes (**2a** and **2d**) and the trichloro Co–Ru–Co sandwich **4**; in addition, the dichloro Co–Co–Co system **3a** was found to be isomorphous with **2a**. The unit cell of **2d** contains a disordered molecule of CH_2Cl_2 in four symmetry-related positions. Information relevant to the crystals, data collection, and data processing are presented in Table IV,

(17) (a) Edwin, J.; Bochmann, M.; Boehm, M. C.; Brennan, D. E.; Geiger, W. E., Jr.; Kruger, C.; Pebler, J.; Pritzkow, H.; Siebert, W.; Swiridoff, W.; Wadepohl, H.; Weiss, J.; Zenneck, U. *J. Am. Chem. Soc.* **1983**, *105*, 2582. (b) Stephan, M. Personal communication.

(18) Pipal, J. R.; Grimes, R. N. Manuscript in preparation.

(19) (a) Merkert, J.; Davis, J. H., Jr.; Grimes, R. N.; Geiger, W. *Abstracts of Papers*, 199th National Meeting of the Americal Chemical Society, Boston, MA, April 1990; American Chemical Society: Washington, DC, 1990; INOR 92. (b) Merkert, J.; Davis, J. H., Jr.; Geiger, W.; Grimes, R. N. *J. Am. Chem. Soc.*, in press.

(20) Jemmis, E. D.; Reddy, A. C. *J. Am. Chem. Soc.* **1990**, *112*, 722.

Table V. Bond Distances and Selected Bond Angles for $[Cp^*Co(Et_2C_2B_3H_2Cl)]_2Ni$ (**2a**)

Bond Distances (Å)			
Ni–C2	2.157 (4)	Co2–C2R5	2.041 (5)
Ni–C3	2.114 (4)	Co2–B9	2.081 (5)
Ni–C7	2.174 (4)	Co2–B10	2.042 (6)
Ni–C8	2.108 (4)	Co2–B11	2.102 (5)
Ni–B4	2.082 (5)	Cl1–B5	1.796 (5)
Ni–B5	2.078 (5)	Cl2–B10	1.802 (6)
Ni–B6	2.143 (5)	C2M–C2	1.504 (6)
Ni–B9	2.075 (5)	C2M–C2E	1.491 (8)
Ni–B10	2.079 (5)	C2–C3	1.466 (6)
Ni–B11	2.137 (5)	C2–B6	1.554 (6)
Co1–C2	2.091 (4)	C3M–C3	1.515 (6)
Co1–C3	2.102 (4)	C3M–C3E	1.485 (8)
Co1–C1R1	2.069 (5)	C3–B4	1.559 (6)
Co1–C1R2	2.097 (5)	C7M–C7	1.506 (6)
Co1–C1R3	2.059 (5)	C7M–C7E	1.509 (8)
Co1–C1R4	2.028 (5)	C7–C8	1.482 (5)
Co1–C1R5	2.031 (4)	C7–B11	1.534 (7)
Co1–B4	2.083 (5)	C8M–C8	1.493 (6)
Co1–B5	2.057 (5)	C8M–C8E	1.512 (8)
Co1–B6	2.113 (5)	C8–B9	1.563 (7)
Co2–C7	2.104 (4)	B4–B5	1.743 (7)
Co2–C8	2.111 (4)	B5–B6	1.713 (7)
Co2–C2R1	2.039 (5)	B9–B10	1.739 (7)
Co2–C2R2	2.044 (5)	B10–B11	1.702 (8)
Co2–C2R3	2.088 (6)	⟨Cp*1 C–C⟩	1.419
Co2–C2R4	2.089 (6)	⟨Cp*1 C–Me⟩	1.496
		⟨Cp*2 C–C⟩	1.395
		⟨Cp*2 C–Me⟩	1.516
Bond Angles (deg)			
C3–C2–B6	114.1 (3)	Cl1–B5–B4	128.0 (3)
C2–C3–B4	112.9 (3)	Cl1–B5–B6	128.8 (3)
C3–B4–B5	104.7 (3)	Co1–B5–Cl1	129.4 (3)
B4–B5–B6	103.2 (3)	Ni–B5–Cl1	129.7 (3)
C2–B6–B5	105.0 (3)	C7M–C7–C8	118.6 (4)
C8–C7–B11	112.9 (4)	C7M–C7–B11	128.5 (4)
C7–C8–B9	113.0 (4)	Co2–C7–C7M	131.7 (3)
C8–B9–B10	104.5 (3)	Ni–C7–C7M	131.6 (3)
B9–B10–B11	102.9 (4)	C7–C7M–C7E	115.0 (5)
C7–B11–B10	106.6 (4)	C8M–C8–B9	126.5 (4)
C2M–C2–C3	120.1 (4)	C7–C8–C8M	120.4 (4)
C2M–C2–B6	125.8 (4)	Co2–C8–C8M	132.8 (3)
Co1–C2–C2M	131.2 (3)	Ni–C8–C8M	129.1 (3)
Ni–C2–C2M	131.6 (3)	C8–C8M–C8E	115.0 (5)
C2–C2M–C2E	115.6 (4)	Cl2–B10–B9	128.0 (4)
C3M–C3–B4	126.3 (4)	Cl2–B10–B11	129.0 (4)
C2–C3–C3M	120.8 (4)	Co2–B10–Cl2	131.0 (3)
Ni–C3–C3M	129.1 (3)	Ni–B10–Cl2	127.6 (3)
Co1–C3–C3M	132.8 (3)		
C3–C3M–C3E	115.2 (4)		

Table VI. Bond Distances and Selected Bond Angles for $[Cp^*Co(Et_2C_2B_3H_2C(O)Me)]_2Ni$ (**2d**)

Bond Distances (Å)			
Ni–C2	2.139 (10)	Ni–C3	2.163 (8)
Ni–B4	2.123 (12)	Ni–B5	2.083 (14)
Ni–B6	2.091 (15)	Ni–C7	2.139 (12)
Ni–C8	2.194 (11)	Ni–B9	2.149 (13)
Ni–B10	2.067 (9)	Ni–B11	2.115 (13)
Co1–C2	2.087 (11)	Co1–C3	2.092 (12)
Co1–B4	2.122 (15)	Co1–B5	2.081 (11)
Co1–B6	2.091 (12)	Co1–C1R1	2.058 (12)
Co1–C1R2	2.050 (14)	Co1–C1R3	2.049 (14)
Co1–C1R4	2.068 (13)	Co1–C1R5	2.092 (10)
Co2–C7	2.099 (8)	Co2–C8	2.103 (9)
Co2–B9	2.111 (14)	Co2–B10	2.088 (14)
Co2–B11	2.087 (13)	Co2–C2R1	2.060 (12)
Co2–C2R2	2.055 (9)	Co2–C2R3	2.060 (11)
Co2–C2R4	2.065 (16)	Co2–C2R5	2.081 (14)
C2–C2M	1.516 (15)	C2–C3	1.437 (16)
C2–B6	1.590 (13)	C2M–C2E	1.528 (19)
C3–C3M	1.510 (12)	C3–B4	1.538 (16)
C3M–C3E	1.541 (18)	B4–B5	1.765 (17)
B5–C9	1.563 (15)	B5–B6	1.749 (20)
C9–O1	1.219 (15)	C9–C10	1.529 (19)
C7–C7M	1.523 (14)	C7–C8	1.492 (16)
C7–B11	1.561 (4)	C7M–C7E	1.533 (18)
C8–C8M	1.509 (13)	C8–B9	1.536 (16)
C8M–C8E	1.520 (19)	B9–B10	1.791 (17)
B10–C11	1.554 (14)	B10–B11	1.780 (19)
C11–O2	1.228 (14)	C11–C12	1.514 (19)
C1S–Cl1C	1.741 (36)	C1S–Cl1A	1.911 (27)
C1S–Cl1B	1.930 (31)	C1S–Cl2A	1.695 (36)
C1S–Cl2B	1.566 (37)	C1S–Cl3A	1.544 (33)
C1S–Cl3B	1.758 (31)	Cl1C–Cl1B	2.413 (46)
Cl1C–Cl2A	1.088 (33)	Cl1C–Cl2B	1.917 (56)
Cl1C–Cl3A	2.003 (33)	Cl1C–Cl3B	1.065 (40)
Cl1A–Cl2A	1.924 (28)	Cl1A–Cl3A	0.836 (29)
Cl1B–Cl2B	0.547 (54)	Cl1B–Cl3B	1.532 (47)
Cl2A–Cl3A	1.100 (32)	Cl2A–Cl3B	2.033 (33)
Cl2B–Cl3B	1.048 (59)	⟨Cp*1 C–C⟩	1.421
		⟨Cp*1 C–Me⟩	1.500
		⟨Cp*2 C–C⟩	1.419
		⟨Cp*2 C–Me⟩	1.492
Bond Angles, deg			
C3–C2–B6	113.5 (9)	B9–B10–B11	101.1 (8)
C2–C3–B4	114.9 (8)	B9–B10–C11	128.6 (11)
C3–B4–B5	105.5 (10)	C11–B10–B11	130.1 (10)
B4–B5–B6	101.4 (8)	C7–B11–B10	104.6 (10)
B4–B5–C9	129.8 (11)	B5–C9–C10	119.1 (10)
C9–B5–B6	128.8 (10)	B5–C9–O1	123.3 (11)
C2–B5–B5	104.7 (9)	O1–C9–C10	117.4 (9)
C8–C7–B11	114.7 (9)	B10–C11–O2	123.3 (12)
C8–B9–B10	105.9 (10)	O2–C11–C12	117.8 (9)

bond distances and angles are listed in Tables V–VII, and tables of positional and thermal parameters and mean planes are provided as supplementary material. Figures 1–3 depict the molecular structures, all of which are tetradecker sandwiches having $Cp^*Co^{III}(Et_2C_2B_3H_yX_{3-y})^{2-}$ units coordinated to a central metal ion which is formally in the +4 oxidation state. It is useful to compare these sandwich structures in terms of their common features, particularly the distances and angles involving the four ring planes and three metal atoms in each species (Table VIII). The main points are as follows.

(1) All of the molecules are nonslipped; i.e., the central metal is approximately centered with respect to its coordinated C_2B_3 rings with no appreciable slip-distortion. This is in accordance with calculations that predict slipped structures for tetradeckers having more than 42 valence electrons, but nonslipped geometries for 42 or fewer electrons.[20] However, each stack is significantly bent in the middle as measured by the deviation of the Co–M–Co angle from 180°, that of **4** being ca. 6° greater than the others. This effect can also be seen in the dihedral angle between the C_2B_3 carborane planes (rings 2 and 3), which in complex **4** is twice that found in the other species. (One can also look at the tilt between end planes (the Cp*–Cp* dihedral angle), which is 34° in **4** but only 20° in the other systems.) Steric repulsions between substituents on opposing C_2B_3 ligands are evidently not a major determinant in these structures, as the bending in each case actually *decreases* the interligand distance. The bending of these stacks is clearly of electronic origin and is attributed to unequal overlap between the orbitals of the central metal and those of the ring boron and carbon atoms. The effect is especially pronounced in the 40-electron system **4**; in this complex, the relatively electron-poor ruthenium(IV) atom binds preferentially to boron, which is a better source of electron density than carbon by virtue of its lower electronegativity.

If the ruthenium atom in **4** were replaced by iron, a similar distortion would be expected; in this case, the smaller radius of Fe would cause the middle boron atoms in the C_2B_3 rings to approach very closely, quite possibly leading to fusion of the two $Cp^*Co(Et_2C_2B_3H_3)^{2-}$ units. Interestingly, this is exactly what is observed when we attempt to prepare Co-Fe-Co tetradeckers, as yet unknown: all such efforts thus far have given instead fused or linked products.[15]

(2) There is remarkable uniformity in the metal–ring and metal–metal distances in these complexes, when the difference

Table VII. Bond Distances and Selected Bond Angles for $(Cp^*Co)_2(2,3\text{-}Et_2C_2B_3H_2\text{-}5\text{-}Cl)(2,3\text{-}Et_2C_2B_3H\text{-}4,5[5,6]\text{-}Cl_2)Ru$ (**4**)

	Bond Distances, Å		
Ru–C2	2.392 (5)	Co2–C2R5	2.087 (5)
Ru–C3	2.222 (5)	Co2–B9	2.138 (6)
Ru–C7	2.199 (5)	Co2–B10	2.066 (6)
Ru–C8	2.376 (5)	Co2–B11	2.043 (6)
Ru–B4	2.148 (6)	Cl1–B5	1.800 (6)
Ru–B5	2.123 (6)	Cl2–B6	1.803 (6)
Ru–B6	2.262 (6)	Cl3–B10	1.789 (6)
Ru–B9	2.285 (6)	C2M–C2	1.503 (7)
Ru–B10	2.128 (6)	C2M–C2E	1.532 (8)
Ru–B11	2.128 (6)	C2–C3	1.466 (7)
Co1–C2	2.054 (5)	C2–B6	1.524 (7)
Co1–C3	2.057 (5)	C3M–C3	1.514 (7)
Co1–C1R1	2.060 (5)	C3M–C3E	1.501 (7)
Co1–C1R2	2.100 (5)	C3–B4	1.600 (7)
Co1–C1R3	2.106 (5)	C7M–C7	1.520 (7)
Co1–C1R4	2.082 (5)	C7M–C7E	1.506 (8)
Co1–C1R5	2.059 (5)	C7–C8	1.457 (7)
Co1–B4	2.048 (5)	C7–B11	1.593 (7)
Co1–B5	2.088 (6)	C8–C8M	1.529 (7)
Co1–B6	2.131 (6)	C8–B9	1.552 (7)
Co2–C7	2.063 (5)	C8M–C8E	1.509 (8)
Co2–C8	2.046 (5)	B4–B5	1.782 (8)
Co2–C2R1	2.117 (5)	B5–B6	1.703 (8)
Co2–C2R2	2.100 (5)	B9–B10	1.734 (8)
Co2–C2R3	2.059 (5)	B10–B11	1.771 (8)
Co2–C2R4	2.062 (5)	⟨Cp*1 C–C⟩	1.430
		⟨Cp*1 C–Me⟩	1.492
		⟨Cp*2 C–C⟩	1.429
		⟨Cp*2 C–Me⟩	1.489
	Bond Angles, deg		
C3–C2–B6	112.2 (4)	C7–C8–B9	113.5 (4)
C2–C3–B4	114.5 (4)	C8–B9–B10	105.7 (4)
C3–B4–B5	102.1 (4)	Cl3–B10–B9	131.4 (4)
Cl1–B5–B4	126.3 (4)	Cl3–B10–B11	125.4 (4)
Cl1–B5–B6	131.0 (4)	B9–B10–B11	103.0 (4)
B4–B5–B6	102.3 (4)	C7–B11–B10	102.8 (4)
Cl2–B6–C2	124.3 (4)		
Cl2–B6–B5	126.7 (4)		
C2–B6–B5	108.3 (4)		
C8–C7–B11	114.4 (4)		

in covalent radii of Ru vs Co and Ni (~0.1 Å) is taken into account. Moreover, the Co–C_2B_3 and Co–Cp* metal–centroid distances are very close to those found in triple-decker sandwiches containing $CpCo(C_2B_3)$ or $Cp^*Co(C_2B_3)$ units;[3a,21] for example, in $CpCo(2,3\text{-}MeC_2B_3H_4)CoCp$,[3a] the Co–$C_2B_3$ value is 1.57 Å. The Co–C_2B_3 distances in the tetradeckers (1.55–1.58 Å) are, however, slightly greater than the corresponding vectors in $Cp^*Co(C_2B_3)$ or $CpCo(C_2B_3)$ double-decker sandwiches;[1a,14c,22] weaker cobalt–carborane ring interactions in the tetradecker complexes would be expected, since electron density in the C_2B_3 rings is involved in bonding to two metals simultaneously. The Co–Cp* distances in Table VI are virtually identical to those of the cobaltocenium ion,[23] $Cp^*_2Co^+$.

(3) The rotational twist angle of the carborane rings, measured as the dihedral angle between the Co–B(5)–M and Co–B(10)–M planes, varies considerably, from 27° in the Co–Ni–Co diacetyl species to 75° in the Co–Ni–Co dichloro complex and 89° in the ruthenium trichloro sandwich. The corresponding angle, which would be zero in a perfectly eclipsed sandwich, varies even more widely in comparable bis(carboranyl) sandwiches of the type $M(R_2C_2B_4H_4)_2$ which have no constraining groups (such as other ligands on the metal) and whose carborane units presumably can rotate freely. Thus, in the complex $H_2Fe(Me_2C_2B_4H_4)_2$ the rotation[24] is 90°, whereas in $Cr[(SiMe_3)_2C_2B_4H_4]_2{}^-$[25] it is 180°. In contrast, the complex $(Me_2C_2B_3H_5)Co(Me_2C_2B_4H_4)^-$ has essentially eclipsed carborane rings.[26] Clearly, these solid-state orientations are highly sensitive to the electronic structure, and in all probability to crystal packing effects as well.

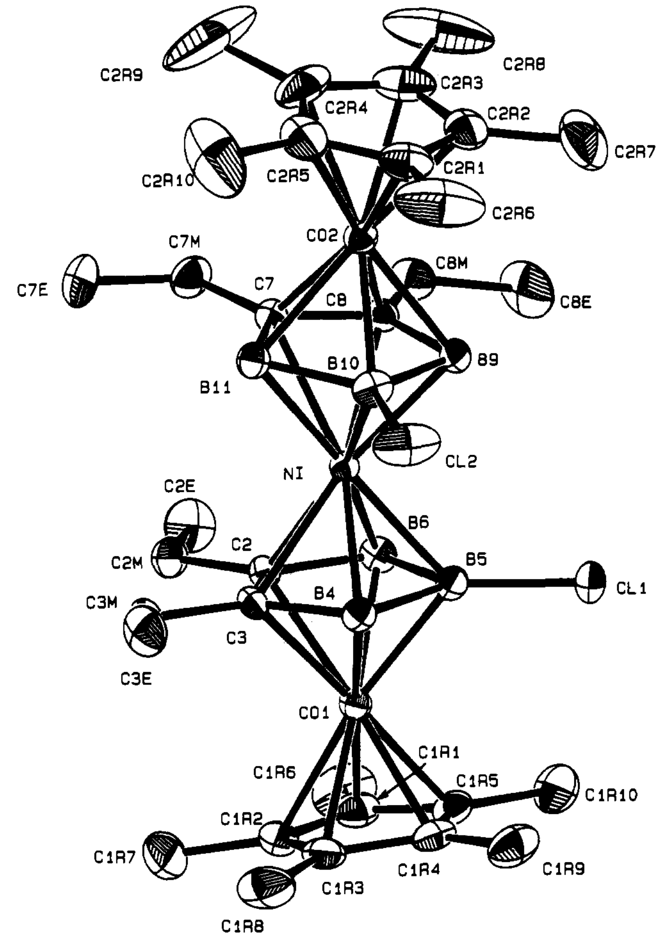

Figure 1. Molecular structure of $[Cp^*Co(2,3\text{-}Et_2C_2B_3H_2\text{-}5\text{-}Cl)]_2Ni$ (**2a**) with 30% probability ellipsoids. Hydrogen atoms are omitted for clarity.

Concluding Remarks

Tetradecker sandwich complexes are of interest in respect to their synthesis, mechanisms of formation from double-decker units, electronic structure, and molecular geometry. In our initial investigation, we have addressed each of these aspects and gained some limited insight into this relatively unexplored area, but work currently in progress is expected to provide a deeper understanding of carborane-based multidecker stacks as well as a clearer picture of the synthetic possibilities. We are currently exploring the use of the tetradecker stacking reaction in assembling large oligomers and polymers,[27] including electroactive materials, and will report on these studies in due course.

(21) (a) Robinson, W. T.; Grimes, R. N. *Inorg. Chem.* **1975**, *14*, 3056. (b) Pipal, J. R.; Grimes, R. N. *Inorg. Chem.* **1978**, *17*, 10. (c) Davis, J. H., Jr.; Sinn, E.; Grimes, R. N. *J. Am. Chem. Soc.* **1989**, *111*, 4776. (d) Davis, J. H., Jr.; Sinn, E.; Grimes, R. N. *Ibid.* **1989**, *111*, 4784.

(22) (a) Piepgrass, K. W.; Davis, J. H., Jr.; Sabat, M.; Grimes, R. N. *J. Am. Chem. Soc.* **1991**, *113*, 680. (b) Finster, D. C.; Grimes, R. N. *Inorg. Chem.* **1981**, *20*, 863. (c) Pipal, J. R.; Maxwell, W. M.; Grimes, R. N. *Ibid.* **1978**, *17*, 1447. (d) Borodinsky, L.; Sinn, E.; Grimes, R. N. *Ibid.* **1982**, *21*, 1928.

(23) (a) Miller, J. S.; Calabrese, J. C.; Harlow, R. L.; Dixon, D. A.; Zhang, J. H.; Reiff, W. M.; Chittipeddi, S.; Selover, M. A.; Epstein, A. J. *J. Am. Chem. Soc.* **1990**, *112*, 5496. (b) Dixon, D. A.; Miller, J. S. *J. Am. Chem. Soc.* **1987**, *109*, 3656.

(24) Pipal, J. R.; Grimes, R. N. *Inorg. Chem.* **1979**, *18*, 263.

(25) Oki, A. R.; Zhang, H.; Maguire, J. A.; Hosmane, N. S.; Ro, H.; Hatfield, W. E. *Organometallics* **1991**, *10*, 2996.

(26) Pipal, J. R.; Maxwell, W. M.; Grimes, R. N. *Inorg. Chem.* **1978**, *17*, 1447.

(27) (a) Meng, X.; Sabat, M.; Grimes, R. N. Submitted for publication. (b) Meng, X.; Grimes, R. N. *Abstracts of Papers*; IX FECHEM Conference on Organometallic *Chemistry*, Heidelberg, Germany, July 1991; Abstract O-21.

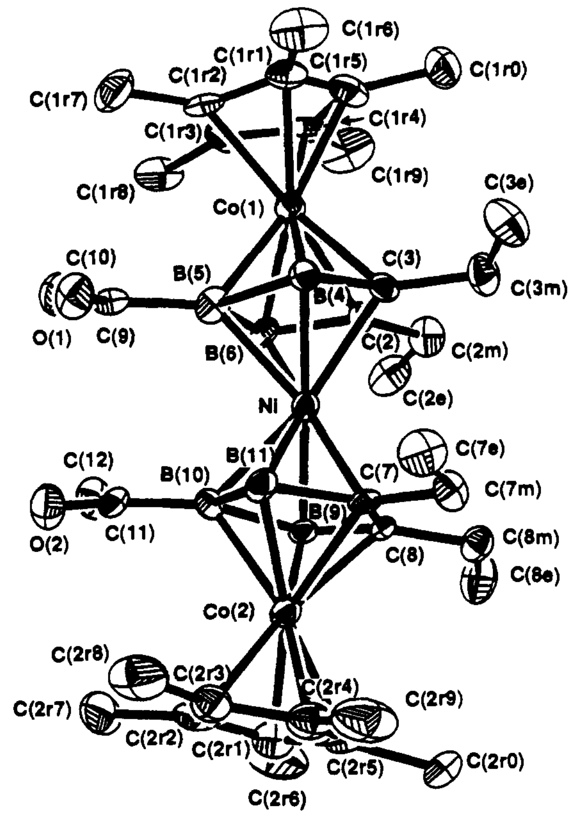

Figure 2. Molecular structure of $[Cp^*Co(2,3\text{-}Et_2C_2B_3H_2\text{-}5\text{-}C(O)Me)]_2Ni$ (**2d**).

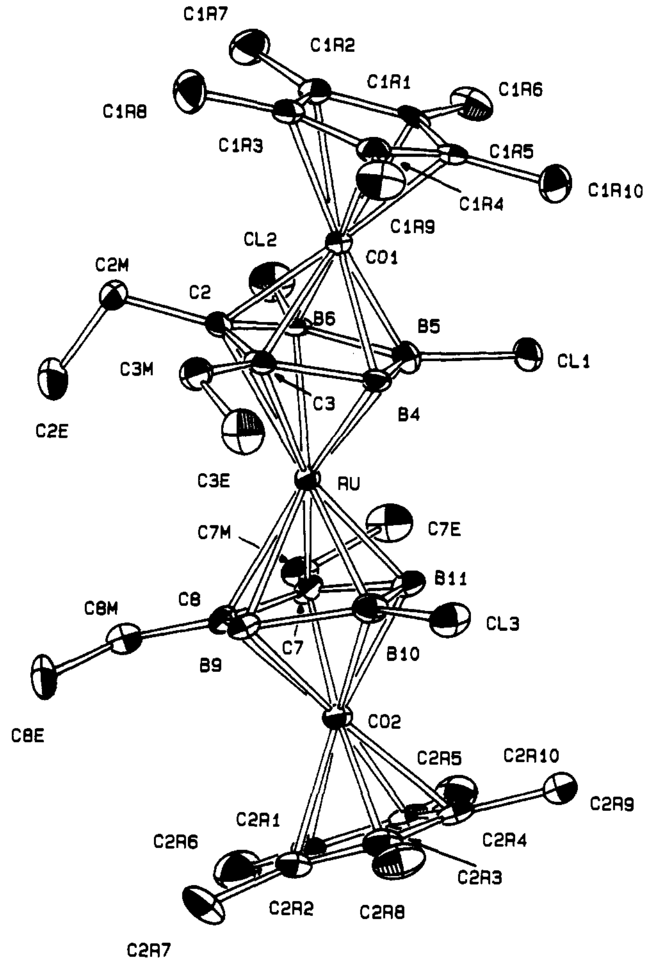

Figure 3. Molecular structure of $(Cp^*Co)_2(2,3\text{-}Et_2C_2B_3H_2\text{-}5\text{-}Cl)(2,3\text{-}Et_2C_2B_3H\text{-}4,5[5,6]\text{-}Cl_2)Ni$ (**4**).

Experimental Section

Instrumentation. ^{11}B (115.8 MHz), ^{13}C (75.5 MHz), and ^{1}H (300 MHz) NMR spectra were acquired on Nicolet NT-360 or GE QE300 spectrometers, and visible–ultraviolet spectra were recorded on a Hewlett-Packard 8452A diode array spectrophotometer with an HP Vectra computer interface. Unit-resolution mass spectra were obtained on a Finnegan MAT 4600 GC/MS spectrometer using perfluorotributylamine (FC43) as a calibration standard. Simulated mass spectra based on natural isotopic abundances were calculated on an AT&T 3B5 computer. In all cases, strong parent envelopes were observed, and the calculated and observed unit-resolution spectral patterns were in close agreement. High-resolution mass measurements were obtained on a Finnegan MAT 8230 instrument using an SSX 300 data system with perfluorokerosene as a reference standard. Elemental analyses were obtained by the E+R Microanalytical Laboratory, Inc., Corona, NY. ESR spectra were recorded on a Varian E3 spectrometer fitted with an electrolytic cell or an Oxford Instruments ESR 300E instrument. Column chromatography was conducted on silica gel 60 (Merck), and thick-layer chromatography was carried out on precoated silica gel plates (Merck).

Materials and Procedures. Dichloromethane and *n*-hexane were anhydrous grade and were stored over 4-Å molecular sieves prior to use (in most syntheses reported herein, solvent drying proved unnecessary). THF was distilled from sodium–benzophenone immediately prior to use. The *nido*-$Cp^*Co(Et_2C_2B_3H_4\text{-}5\text{-}X)$ complexes **1a**–**1f** were prepared as described elsewhere.[14] Except where otherwise indicated, all syntheses were conducted under vacuum or an atmosphere of nitrogen. Workup of products was generally conducted in air using benchtop procedures.

Synthesis of $[Cp^*Co(2,3\text{-}Et_2C_2B_3H_2\text{-}5\text{-}Cl)]_2Ni$ (2a). The 5-chloro complex **1a** (180 mg, 0.52 mmol) was placed in a 3-neck 100-mL flask which was fitted with a septum and attached to a vacuum line. Nickel(II) bromide (58 mg, 0.27 mmol) was placed in a tip tube and attached to the third neck. About 60 mL of dry THF was condensed into the reactor in a liquid nitrogen bath under vacuum, and the flask was warmed to ice–water temperature. To this solution was added, via syringe, an equimolar amount of *tert*-butyllithium in hexane (0.31 mL, 0.53 mmol). The solution immediately turned orange and was warmed to room temperature with no further color change. After 30 min, the solution was cooled to 0 °C and the $NiBr_2$ was tipped in; the color changed slightly to light brown, but most of the $NiBr_2$ did not dissolve at this temperature. The solution was again warmed to room temperature and the color became darker as it warmed; within 30 min the solution was black. After being stirred for 3.5 h, the reactor was opened to the air and the solvent was removed. The dark brown-black residue was washed with hexane to give a yellow solution and a dark brown insoluble solid. The solution was column-chromatographed in hexane to give a yellow band of recovered **1a** (94 mg, 52%). The brown solid was taken up in CH_2Cl_2, filtered through 2 cm of silica, and evaporated to dryness. The residue was taken up in 1:1 hexane–CH_2Cl_2 and column-chromatographed in the same solvent, yielding two dark brown bands. The first band was a mixture of **1a** and the triple-decker complex $Cp^*Co(Et_2C_2B_3H_2Cl)CoCp^*$. The second band gave, on evaporation of solvent, dark brown crystals of **2a** (60 mg, 0.080 mmol, 65% yield based on **1a** consumed). Exact mass: calcd for $^{60}Ni^{59}Co_2{}^{37}Cl_2{}^{12}C_{32}{}^{11}B_6{}^{1}H_{54}{}^{+}$, 756.2074; found, 756.2107.

Synthesis of $[Cp^*Co(2,3\text{-}Et_2C_2B_3H_2\text{-}5\text{-}Br)]_2Ni$ (2b). In a procedure analogous to the preceding synthesis, a solution of $\mathbf{1b}^-$ ion in THF solution was prepared via deprotonation of **1b** (170 mg, 0.43 mmol) with butyllithium in THF, and nickel(II) bromide (47 mg, 0.22 mmol) was added. Workup was conducted as before, with the residue taken up in CH_2Cl_2 and the solution washed through 2 cm of silica and column-chromatographed, first with hexane, which afforded 47 mg (28% recovery) of **1b** and an orange band consisting of several unidentified species. Elution of the column with 1:1 hexane–CH_2Cl_2 gave a dark brown band which on evaporation gave crystals of **2b** (49 mg, 0.058 mmol, 38% based on **1b** consumed).

Synthesis of $[Cp^*Co(2,3\text{-}Et_2C_2B_3H_2\text{-}5\text{-}Me)]_2Ni$ (2c). The same procedure was followed by employing the *B(5)*-methyl complex **1c** (0.206 g, 0.63 mmol) and 70 mg (0.32 mmol) of $NiBr_2$. The hexane wash gave recovered **1c** (0.107 g, 52%). The residue from the CH_2Cl_2 wash was chromatographed on silica plates with 1:1 CH_2Cl_2–hexane, giving two bands of which the second was dark brown **2c** (45 mg, 0.063 mmol, 42% based on **1c** consumed).

Synthesis of $[Cp^*Co(2,3\text{-}Et_2C_2B_3H_2\text{-}5\text{-}C(O)Me)]_2Ni$ (2d). The *B(5)*-acetyl derivative **1d** (0.192 g, 0.54 mmol) was deprotonated and treated with 60 mg (0.27 mmol) $NiBr_2$ as before. The hexane wash was chromatographed on silica plates, giving several bands of which the largest

Table VIII. Comparison of Tetradecker Sandwich Structures

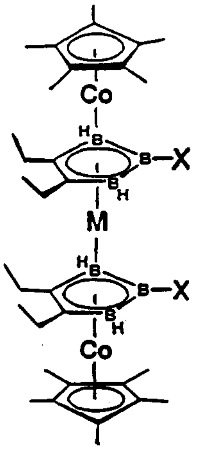
1
2
3
4

	Co–Ni–Co dichloro (**2a**)[a]	Co–Ni–Co diacetyl (**2d**)	Co–Ru–Co trichloro (**4**)
Co–M–Co angle, deg	172	171	165
dihedral angles, deg			
ring 1–ring 2	6.4	4.5	5.0
ring 2–ring 3	9.4	11.8	22.1
ring 3–ring 4	5.1	3.7	6.6
ring 1–ring 4	20.4	20.0	33.7
rotational twist,[b] deg	75	27	89
Co–M dist, Å	3.19, 3.19	3.18, 3.19	3.30, 3.30
C2–C3 and C7–C8 dist, Å	1.47, 1.48	1.44, 1.49	1.47, 1.46
$M–C_2B_3$ dist,[c] Å	1.61, 1.62	1.62, 1.62	1.76, 1.75
$Co–C_2B_3$ dist,[c] Å	1.58, 1.58	1.57, 1.58	1.56, 1.55
$Co–C_5Me_5$ dist,[c] Å	1.67, 1.68	1.67, 1.68	1.69, 1.69

[a] Isomorphous with the Co–Co–Co dichloro complex (**3a**). [b] Dihedral angle between Co–B5–M and Co–B10–M planes. [c] Metal–ring centroid vectors.

was recovered **1d** (61 mg, 32%). The silica was stripped with methanol, the eluent was evaporated to dryness, and the residue was taken up in 1:1 CH_2Cl_2–acetonitrile and chromatographed on a silica column in that solvent. A small yellow band was followed by a major brown band which was **2d** (58 mg, 0.076 mmol, 41% based on **1d** consumed). Exact mass: calcd for $^{60}Ni^{59}Co_2{}^{16}O_2{}^{12}C_{36}{}^{11}B_6{}^{1}H_{60}{}^{+}$, 768.3124; found, 768.3143.

Synthesis of [Cp*Co(2,3-$Et_2C_2B_3H_2$-5-$CH_2C{\equiv}CMe$)]$_2$Ni (2e). The same procedure was followed with the *B*(*5*)-(2-butynyl) complex **1e** (0.208 g, 0.57 mmol), employing 63 mg (0.29 mmol) of $NiBr_2$. The hexane wash contained only stopcock grease. The residue from the CH_2Cl_2 wash was column-chromatographed in 1:1 CH_2Cl_2–hexane, affording a red band which was evaporated to give a red oil identified as **1e** (59 mg, 28%). Several small bands were then eluted, followed by a dark brown band, which on evaporation yielded **2e** (17 mg, 0.022 mmol, 11% based on **1e** consumed). Exact mass: calcd for $^{60}Ni^{59}Co_2{}^{12}C_{40}{}^{11}B_6{}^{1}H_{64}{}^{+}$, 788.3538; found, 788.3530.

Synthesis of [Cp*Co(2,3-$Et_2C_2B_3H_2$-5-Cl)]$_2$Co (3a). The method described for the preparation of **2a** was followed with 37 mg (0.28 mmol) of $CoCl_2$ and 0.197 g (0.57 mmol) of **1a**. The hexane wash yielded 0.104 g (52% recovery) of **1a**. Column chromatography of the residue dissolved in 1:1 CH_2Cl_2–hexane gave several bands, of which the third and largest gave, on evaporation, dark brown crystals of **3a** (70 mg, 0.093 mmol, 69% based on **1a** consumed). Exact mass: calcd for $^{59}Co_3{}^{37}Cl_2{}^{12}C_{32}{}^{11}B_6{}^{1}H_{54}{}^{+}$, 755.2098; found, 755.2059.

Synthesis of [Cp*Co(2,3-$Et_2C_2B_3H_2$-5-Br)]$_2$Co (3b). The procedure used to prepare **2b** was followed using 0.208 g (0.53 mmol) of **1b** and 58 mg (0.27 mmol) of $CoBr_2$ ($CoCl_2$ cannot be used as it generates exclusively the chlorinated tetradecker). The hexane wash gave recovered **1b** (0.106 g, 50%). The dichloromethane fraction, following chromatography with 1:1 CH_2Cl_2–hexane, afforded dark brown crysals of **3b** (78 mg, 0.093 mmol, 72% based on **1b** consumed). Anal. Calcd for $Br_2Co_3C_{32}B_6H_{54}$: C, 45.74; H, 6.48. Found: C, 45.82; H, 6.60.

Synthesis of [Cp*Co(2,3-$Et_2C_2B_3H_2$-5-Me)]$_2$Co (3c). The method used in the synthesis of **2c** was employed with 0.401 g (1.22 mmol) of **1c** and 79 mg (0.61 mmol) of $CoCl_2$. The hexane wash contained only **1c** (0.186 g, 46%). The dichloromethane wash was column-chromatographed in 1:1 CH_2Cl_2–hexane to give a single dark brown band, which on evaporation afforded dark brown crystalline **3c** (0.143 g, 0.020 mmol, 61% based on **1c** consumed. Anal. Calcd for $Co_3C_{34}B_6H_{60}$: C, 57.48; H, 8.51. Found: C, 57.63; H, 8.72.

Synthesis of [Cp*Co(2,3-$Et_2C_2B_3H_2$-5-C(O)Me)]$_2$Co (3d). The procedure employed for **2d** was followed using 0.163 g (0.46 mmol) of **1d** and 59 mg (0.46 mmol) of $CoCl_2$. Workup as before gave 10 mg of recovered **1d**, 57 mg (23%) of the red-brown triple-decker complex Cp*Co-($Et_2C_2B_3H_2$-5-C(O)Me)CoCp* (identified by proton NMR and mass spectroscopy), and 18 mg (0.024 mmol, 10%) of **3d**.

Synthesis of [Cp*Co(2,3-$Et_2C_2B_3H_2$-5-$CH_2C{\equiv}CMe$)]$_2$Co (3e). The procedure employed in preparing **2e** was followed, using 58 mg (0.27 mmol) of $CoCl_2$ and 0.196 g (0.54 mmol) of **1e**. The hexane wash contained 53 mg (27%) of recovered **1e**. The residue from the CH_2Cl_2 wash was column-chromatographed in 1:1 CH_2Cl_2–hexane, giving four dark brown bands, each of which was evaporated to give dark brown crystals. Unit resolution mass spectra of these compounds gave parent masses of *m/z* 786, 787, 788, and 789, respectively. The *m/z* 786 material was **3e** (7 mg, 0.01 mmol, ca. 5% based on **1e** consumed). The largest band was the *m/z* 787 complex, presumably [Cp*Co(2,3-$Et_2C_2B_3H_2$-5-$CH_2C{\equiv}CMe$)]$_2$CoH (i.e., **3e** with an additional hydrogen), 37 mg (0.047 mmol, 10%). Anal. Calcd for $Co_3C_{40}B_6H_{64}$ (**3e**): C, 61.08; H, 8.20. Found: C, 60.85; H, 8.40.

Synthesis of [Cp*Co(2,3-$Et_2C_2B_3H_3$)]$_2$Co (3f). Cobalt(II) chloride (1.20 g, 9.2 mmol) was placed in a 3-neck flask (A) equipped with a septum and attached to a vacuum line. A two-neck flask (B), was fitted with a septum, was attached to the first flask by a greased ground-glass connector, and in it was placed 2.725 g (8.7 mmol) of the parent complex Cp*Co(2,3-$Et_2C_2B_3H_5$) (**1f**). Both flasks were evacuated, and dry THF was distilled into each. A solution of 9.0 mmol of NaCp* in hexane was added via the septum to flask A, and the mixture was stirred for 4 h. At this point *n*-butyllithium (8.7 mmol) was added to flask B at 0 °C, and this solution was stirred at room temperature for 1 h. Flask B was rotated on its connecting tube and its contents added to flask A. The mixture was stirred for 4 h, after which the solution was opened to the air, solvent was removed by evaporation, and the residue was dried in vacuo. The residue was taken up in hexane, and a portion of this solution was chromatographed on a silica column to give two yellow bands, which were the coupled complexes[15] [Cp*Co($Et_2C_2B_3H_3$)]$_2$ and [Cp*Co-($Et_2C_2B_3H_4$)]$_2$ in yields of 10 and 24%, respectively, together with the red-brown triple-decker species Cp*Co($Et_2C_2B_3H_3$)CoCp (ca. 25%) and 1.427 g (52% recovery) of the starting material **1f**. The hexane-insoluble portion was dissolved in CH_2Cl_2, and the solution was concentrated to saturation point and stored in a refrigerator for several days, which afforded black cubic crystals of **3f** (0.397 g, 0.584 mmol, 28% based on **1f** consumed). Compound **3f** is stable indefinitely in the solid state, but in solution it decomposes on exposure to air or silica. Anal. Calcd for $Co_3C_{32}B_6H_{56}$ (**3f**): C, 56.32; H, 8.27. Found: C, 56.36; H, 8.21.

Synthesis of (Cp*Co)$_2$(2,3-$Et_2C_2B_3H_2$-5-Cl)(2,3-$Et_2C_2B_3H$-4,5[5,6]-Cl_2)Ru (4). The *B*(*5*)-chloro complex **1a** (0.311 g, 0.89 mmol) was deprotonated with butyllithium in THF as in the preceding syntheses, and 0.125 g (0.45 mmol) of $RuCl_2(1,5\text{-}C_8H_{12})$ was added very slowly in vacuo via a tip tube. The mixture was stirred overnight, and the solution was opened to the air, the solvent stripped off, and the residue taken up in CH_2Cl_2 and chromatographed on silica. Three bands were obtained, and the third, red-brown, band was collected, redissolved in 1:3 CH_2Cl_2–hexane, and placed on a silica gel column. Elution with 95:5 hexane–Et_2O gave three bands, of which the third, characterized as **4** (70 mg, 0.085 mmol, ca. 20% yield based on **1a** employed), was the most cleanly separated. Analytically pure samples of this compound were difficult to obtain, the main contaminants being apparently other chlorinated tetradecker Co–Ru–Co complexes, as shown by mass spectra. However, repeated chromatography afforded a small quantity that was sufficient for obtaining NMR spectra and for growing crystals for X-ray data collection.

X-ray Structure Determinations. Measurements on compound **2a** were carried out on a Nicolet P3m diffractometer at 25 °C, those on **3a** were obtained on a Siemens R3m/V diffractometer at −120 °C, and those on **4** were collected on a Rigaku AFC6S instrument at −120 °C, in all cases using Mo Kα radiation. Table IV lists information on the data collections, crystal parameters, and structure determinations. For each structure, full-matrix least-squares calculations with anisotropic thermal displacement parameters for all nonhydrogen atoms yielded the final values of R and R_w given in Table IV. For **2a**, cell dimensions were obtained using 20 high-angle reflections, and the intensities of three standard reflections were checked every 3 h of X-ray exposure. No significant variation in their intensities was observed. The structure was solved by direct methods in TEXSAN 5.0.[28] Hydrogen atoms were located from difference Fourier maps and included as fixed contributions to the structure factors. The final difference Fourier map was featureless.

For **2d**,[29] preliminary measurements suggested a triclinic unit cell. Cell dimensions were determined using 25 high-angle reflections, and the intensities of three standard reflections were checked every 3 h of X-ray exposure, with no significant variation in their intensities. The structure was solved by direct methods in the SHELXTL PLUS[30] package. Hydrogen atoms were placed in calculated positions and included as fixed contributions to the structure factors. The final difference Fourier map was featureless.

For **4**, lattice parameters were determined by least-squares refinement of the setting angles of 25 high-angle reflections, and the intensities of three standard reflections were measured every 100 reflections. The intensities were corrected for absorption based on azimuthal scans of six reflections with transmission factors as given in Table IV. The structure was solved by direct methods (SIR88).[31] All hydrogen atoms except that attached to B(9) were located from difference Fourier maps and introduced into the calculations without refinement. During the final stages of refinement, a difference map showed a density peak ca. 2 e $Å^{-3}$ high at a distance of 1.60 Å from B(9); this was assumed to represent a partially populated ($\sim$10%) site occupied by another chlorine atom [Cl(4)]. The Cl(4) atom was refined with an isotropic thermal parameter. The largest residual peak in the final difference map was 0.59 e $Å^{-3}$ high.

Acknowledgment. This work was supported by the U. S. Army Research Office and the National Science Foundation, Grant No. CHE 9022713. We thank Professor J. R. Pipal for repurifying a sample of the ruthenium complex **4** and obtaining NMR spectra on that compound and Professor Jim Davis for the initial preparation of the diacetyl tetradecker **2d**. M.H. thanks Professor Peter Paetzold of the Institut für Anorganische Chemie, Technischen Hochschule Aachen, Germany, for financial support during his work at the University of Virginia.

Supplementary Material Available: Tables of positional and isotropic thermal parameters, anisotropic thermal parameters, mean planes, and bond distances and angles in the Cp* ligands (18 pages). Ordering information is given on any current masthead page.

(28) TEXSAN 5.0: TEXRAY Structure Analysis Package, Molecular Structure Corp., The Woodlands, TX; 1989.
(29) We are grateful to Dr. Charles F. Campana of the Siemens Corp., Madison, WI, for assistance with the X-ray data collection on this compound.
(30) SHELXTL PLUS: Siemens Analytical X-Ray Instruments Inc., Madison, WI, 1990.
(31) SIR88: Burla, M. C.; Camalli, M.; Cascarano, G.; Giacovazzo, C.; Polidori, G.; Spagna, R.; Viterbo, D. *J. Appl. Crystallogr.* **1989**, *22*, 389.